Article:
Wallis, BJ, Hogg, AE orcid.org/0000-0002-6441-4937, van Wessem, JM et al. (2 more authors) (2023) Widespread seasonal speed-up of west Antarctic Peninsula glaciers from 2014 to 2021. Nature Geoscience, 16 (3). pp. 231-237. ISSN 1752-0894

https://doi.org/10.1038/s41561-023-01131-4

Widespread seasonal speed-up of West Antarctic Peninsula glaciers from 2014 to 2021:

Additional Data

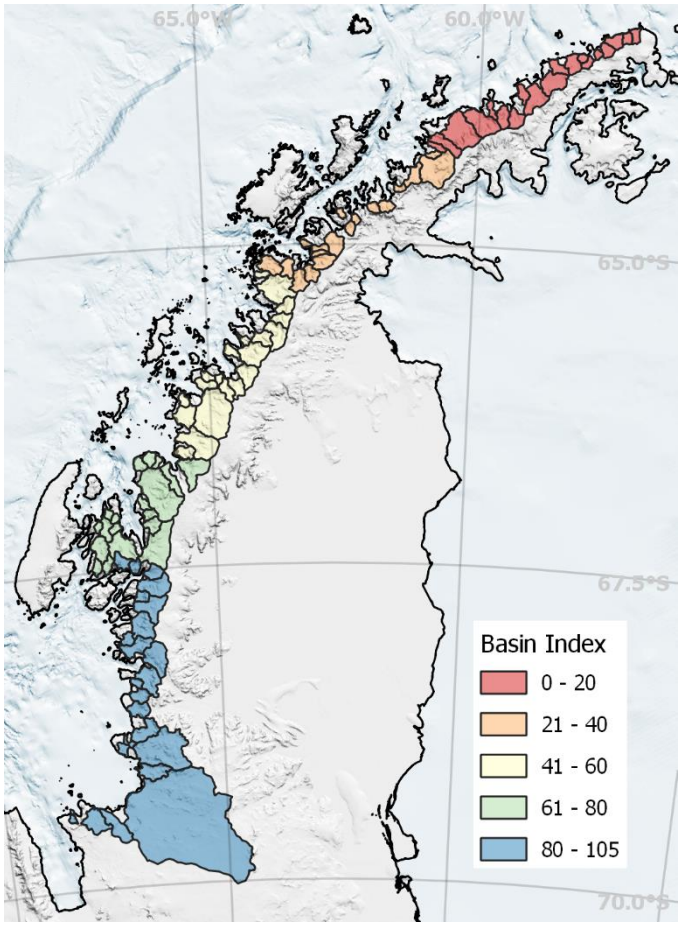

Figure S1 *- Map of west Antarctic Peninsula (AP) glacier drainage basin ID's[70], numbered 1 to 105 running from north to south. The REMA Antarctica 200 m DEM hill shade, coastline (black line) and bathymetry from IBCSO v1 are also shown[71,72].*

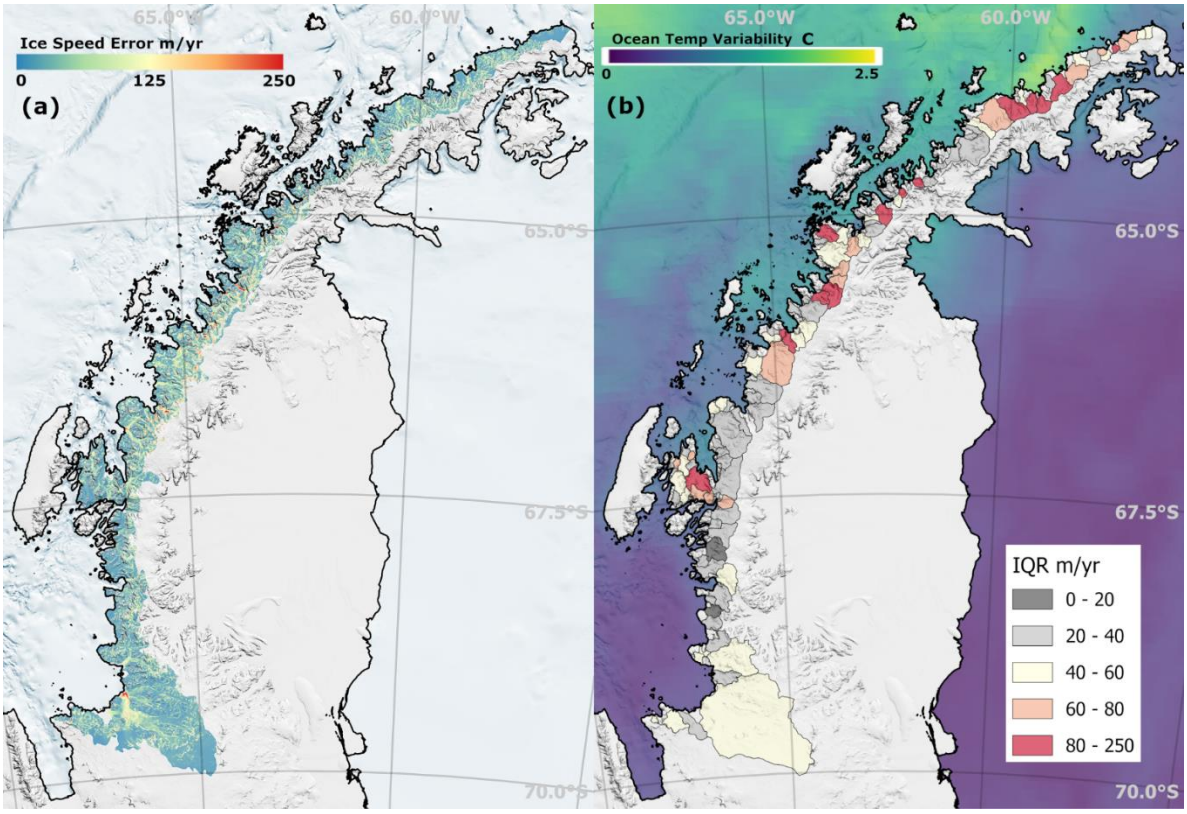

Figure S2 *– a) Ice velocity error map (m/yr) on the west AP and b) Glacier drainage basins[70] shaded by the mean annual ice velocity interquartile range (IQR), which indicates high amplitude (red) and low amplitude (light grey) variability. Inter-annual upper ocean temperature variation is also shown, measured as the annual interquartile range of the depth averaged temperature anomaly in the top 110 m of the water column[56]. The REMA Antarctica 200 m DEM hill shade[71], coastline (black line) and bathymetry from IBSCO v1[72] is shown on both maps.*

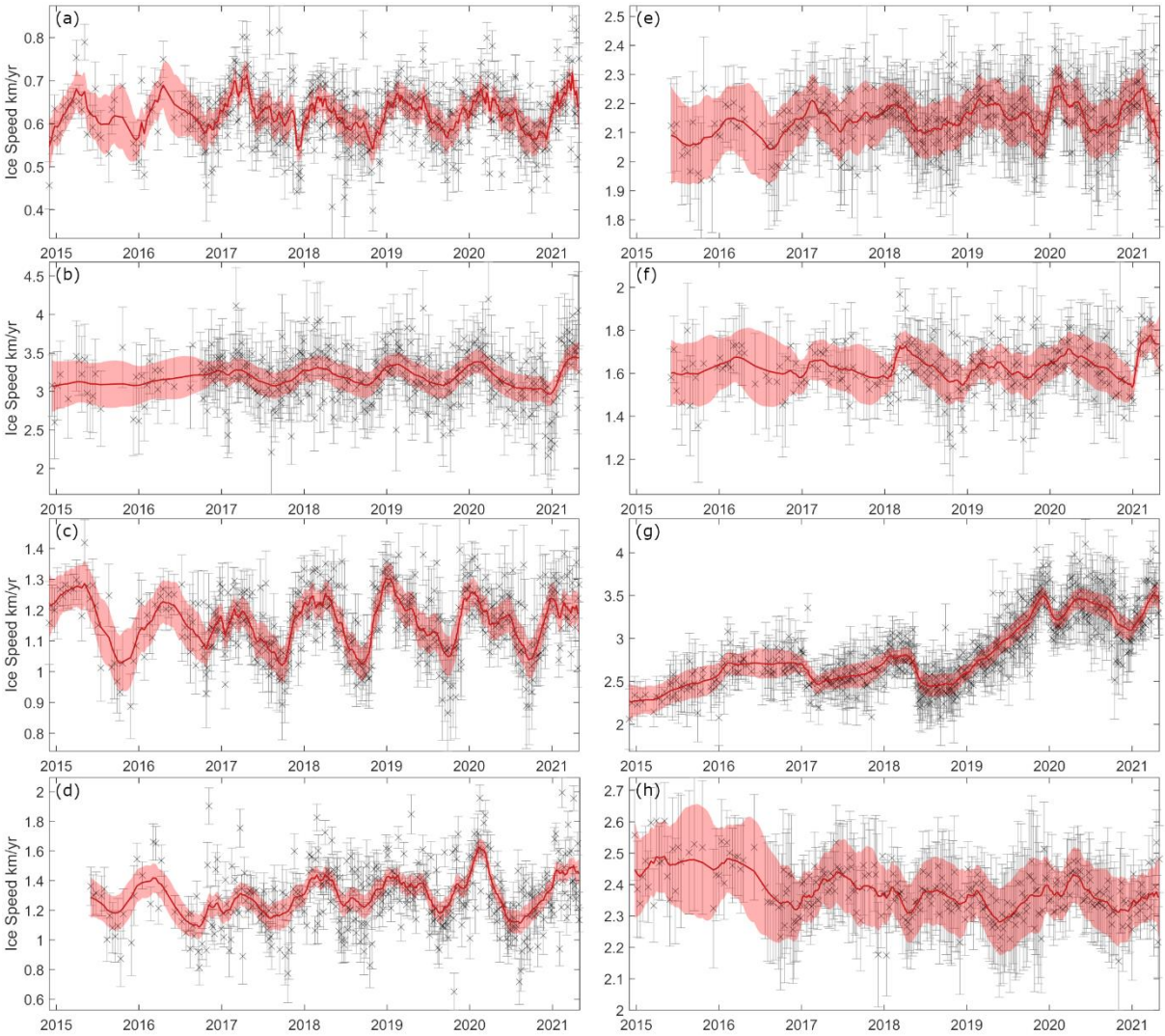

Figure S3 *– Time-series of ice speed for 8 highlight glaciers (Fig. 2a-h). Velocity tracking measurements from individual image pairs are shown as grey cross and whiskers, where the central cross is the magnitude of the velocity measurement and the central date of the image pair, and the error bar is the ice velocity tracking error defined by Lemos et al. 2018 (see Methods). Red line and shading show the Kalman smoothed speed estimate (red line) with its 95% confidence interval (light red shaded area). Time-series are shown for: a) unnamed North Bone Bay (Fig. 2a, 9), b) Gavin Ice Piedmont (Fig. 2b, 11), c) Leonardo (Fig. 2c, 27), d) Hotine (Fig. 2d, 39), e) Trooz (Fig. 2e, 42), f) Keith (Fig. 2f, 58), g) Cadman (Fig. 2g, 45) and h) Fleming (Fig. 2h, 100) Glaciers. Glaciers 'a' to 'f' were selected because of their high magnitude seasonal ice speed variability, (autocorrelation values of 0.648, 0.314, 0.586, 0.703, 0.575, 0.575 respectively) while Fleming and Cadman Glaciers were selected because of their recent longer-term ice dynamic change. We showcase a range of mean ice speeds and locations across the west AP.*

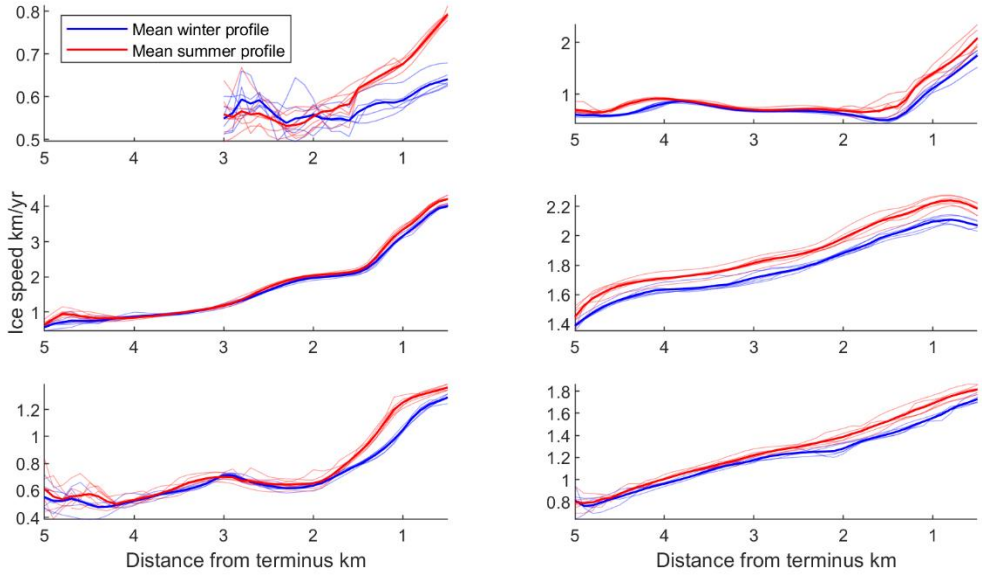

Figure S4 *– Flow-line profile of mean summer (red) and winter (blue) ice speeds, where the 6-year long record of annual speeds (thin line) and the 6-year average (thick line) are both shown. Profiles were extracted when the annual maximum and minimum speeds are measured for each year. Data is shown for 8 highlight glaciers: Flow-line profiles are shown for: a) unnamed North Bone Bay (Fig. 2a, 9), b) Gavin Ice Piedmont (Fig. 2b, 11), c) Leonardo (Fig. 2c, 27), d) Hotine (Fig. 2d, 39), e) Trooz (Fig. 2e, 42), f) Keith (Fig. 2f, 58). Profiles are shown from 0.5 km to 5 km from the terminus.*

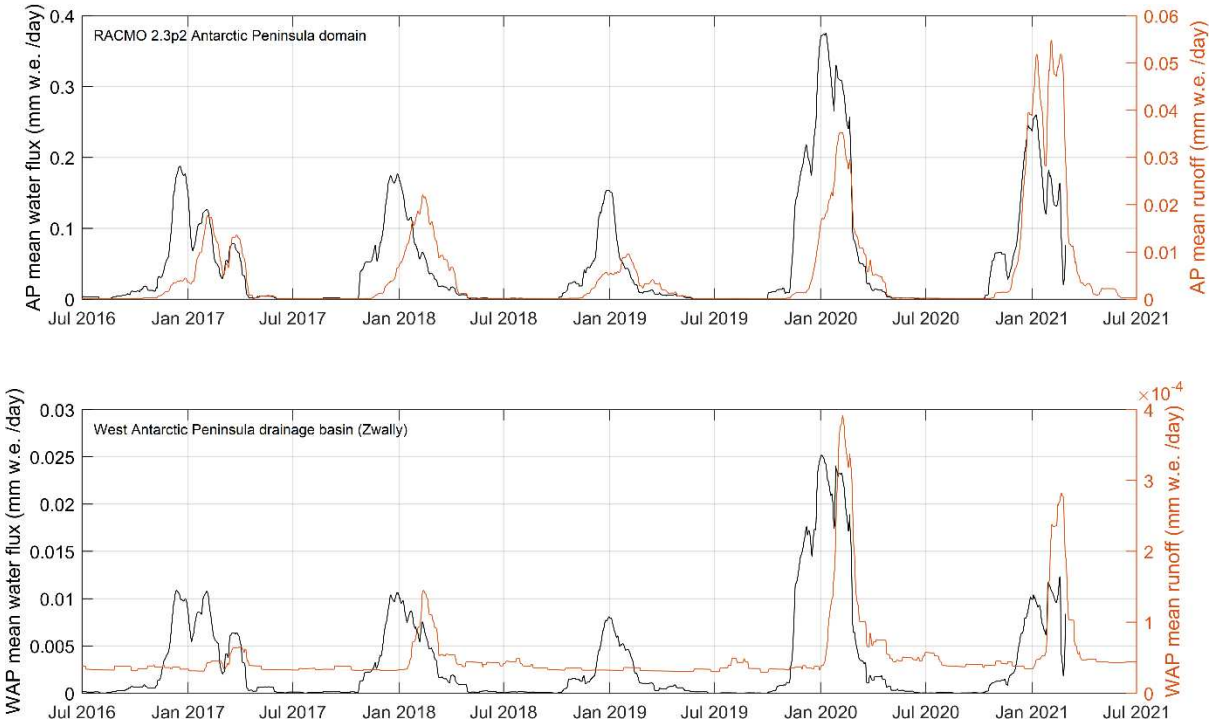

Figure S5 *– Modelled surface water flux (snow-melt plus rain) (black) and water runoff (orange) for RACMO 2.3p2 over the whole model Antarctic Peninsula domain (upper) and the west AP drainage basin[73] (lower*).

Table S1 *– Ice discharge and mass balance for 6 highlight glaciers (Fig 2a-f), when using the annually variable ice speed, and assuming the summer maximum speed is sustained all year. Hotine glacier shares a drainage basin with neighbouring Leay glacier in our dataset, so mass balance is calculated for the whole basin using ice discharge across both outlets. Surface mass balance (SMB) taken from RACMO 2.3p2 AP 5.5 km*[45]*. The error term in ice discharge is dominated by uncertainties in the bed elevation dataset (Huss & Farinotti 2014)*[41] *which are up to 39%. Error terms in SMB are taken from Rignot 2019*[83]*.*

Glacier	Ice Discharge Gt/yr	Ice Discharge with summer speeds Gt/yr	Ice Discharge change	SMB Gt/yr	MB Gt/yr	MB with summer speeds Gt/yr	MB change
a) N. Bone Bay	0.598 ± 0.237	0.625 ± 0.248	-4.58 %	0.520 ± 0.076	-0.078 ± 0.249	-0.105 ± 0.259	35.1 %
b) Gavin Ice Piedmont	1.186 ± 0.473	1.232 ± 0.491	-3.85 %	1.380 ± 0.203	0.194 ± 0.515	0.148 ± 0.531	23.5 %
c) Leonardo	0.352 ± 0.036	0.377 ± 0.039	-6.90 %	0.475 ± 0.070	0.123 ± 0.079	0.099 ± 0.080	19.7 %
d.1) Hotine	0.434 ± 0.176	0.476 ± 0.192	-9.48 %				
d.2) Leay	0.623 ± 0.271	0.698 ± 0.304	-12.12 %				
d) Hotine + Leay	1.057 ± 0.323	1.174 ± 0.357	-11.04 %	1.236 ± 0.182	0.179 ± 0.371	0.062 ± 0.403	65.2 %
e) Trooz	2.578 ± 0.523	2.691 ± 0.552	-4.37 %	1.962 ± 0.288	-0.617 ± 0.603	-0.730 ± 0.623	18.3 %
f) Keith	1.464 ± 0.394	1.511 ± 0.407	- 3.17 %	1.227 ± 0.180	-0.237 ± 0.433	-0.283 ± 0.445	19.6%

References

1. Cook, A. J., Vaughan, D. G., Luckman, A. J. & Murray, T. A new Antarctic Peninsula glacier basin inventory and observed area changes since the 1940s. *Antarct. Sci.* **26**, 614–624 (2014).
2. Arndt, J. E. *et al.* The International Bathymetric Chart of the Southern Ocean (IBCSO) Version 1.0—A new bathymetric compilation covering circum-Antarctic waters. *Geophys. Res. Lett.* **40**, 3111–3117 (2013).
3. Howat, I. M., Porter, C., Smith, B. E., Noh, M.-J. & Morin, P. The Reference Elevation Model of Antarctica. *The Cryosphere* **13**, 665–674 (2019).
4. Jean-Michel, L. *et al.* The Copernicus Global 1/12° Oceanic and Sea Ice GLORYS12 Reanalysis. *Front. Earth Sci.* **9**, 585 (2021).
5. van Wessem, J. M. *et al.* The modelled surface mass balance of the Antarctic Peninsula at 5.5 km horizontal resolution. *The Cryosphere* **10**, 271–285 (2016).
6. Huss, M. & Farinotti, D. A high-resolution bedrock map for the Antarctic Peninsula. *The Cryosphere* **8**, 1261–1273 (2014).
7. Rignot, E. *et al.* Four decades of Antarctic Ice Sheet mass balance from 1979–2017. *Proc. Natl. Acad. Sci.* **116**, 1095–1103 (2019).